

EFFICIENT SHOCK CAPTURING FOR ISENTROPIC FLOWS USING ARITHMETIC AVERAGING

P. GLAISTER

Department of Mathematics, PO Box 220, University of Reading, Reading, RG6 2AX, UK

ABSTRACT

A shock capturing scheme is presented for the equations of isentropic flow based on upwind differencing applied to a locally linearized set of Riemann problems. This includes the two-dimensional shallow water equations using the familiar gas dynamics analogy. An average of the flow variables across the interface between cells is required, and this average is chosen to be the arithmetic mean for computational efficiency, leading to arithmetic averaging. This is in contrast to usual 'square root' averages found in this type of Riemann solver where the computational expense can be prohibitive. The scheme is applied to a two-dimensional dam-break problem and the approximate solution compares well with those given by other authors.

KEY WORDS Isentropic flows Arithmetic averaging Gas dynamics Riemann solver

INTRODUCTION

For many compressible flow simulations the governing equations are assumed to be the Euler equations. However, for some problems, e.g. the flow of natural gas in a pipe, it is sufficient to use the equations of isentropic flow. In particular, using the familiar gas dynamics analogy, the isentropic flow equations give rise to the two-dimensional shallow water equations.

In a recent paper¹ a linearized Riemann solver was presented for the two-dimensional shallow water equations. This work built on the ideas of earlier work on Riemann solvers for the Euler equations of compressible flow^{2,3}. In this paper a new scheme is presented for the equations of isentropic flow, including the two-dimensional shallow water equations, that incorporates the ideas mentioned earlier for the Euler equations and the shallow water equations. There is one distinct difference, however, between the Riemann solver presented here and the Riemann solvers^{1–3}. Riemann solvers of this type require averages of the flow variables across the interface between adjacent computational cells, and a 'square root' average is utilized to make shock (or bore) capturing automatic^{1–3}. In this work, the arithmetic mean is chosen as the required average, whilst still retaining the crucial shock (or bore) capturing property. This results in an efficient scheme which is in contrast to schemes involving the 'square root' whose computational cost can be prohibitive. Although the derivation of this scheme is detailed, its implementation is straightforward. An extension is given for shallow water flows in a channel where friction terms are included and the bottom slope of the channel is non-zero. The resulting algorithm is efficient and produces satisfactory results for a two-dimensional dam-break problem and the results compare well with those given by other authors^{4,5}.

0961–5539/94/040453–11\$2.00

© 1994 Pineridge Press Ltd

Received December 1993

GOVERNING EQUATIONS

The three-dimensional equations of isentropic flow of a compressible fluid can be written in conservation form as:

$$\mathbf{w}_t + \mathbf{F}_x + \mathbf{G}_y + \mathbf{H}_z = \mathbf{0} \quad (1)$$

where

$$\mathbf{w} = (\rho, \rho u, \rho v, \rho w)^T \quad (2a)$$

$$\mathbf{F}(\mathbf{w}) = (\rho u, p + \rho u^2, \rho uv, \rho uw)^T \quad (2b)$$

and

$$\mathbf{G}(\mathbf{w}) = (\rho v, \rho vu, p + \rho v^2, \rho vw)^T \quad (2c)$$

$$\mathbf{H}(\mathbf{w}) = (\rho w, \rho wu, \rho wv, p + \rho w^2)^T \quad (2d)$$

The quantities $(\rho, u, v, w, p)(x, y, z, t)$ represent the density, the velocity in the three coordinate directions, and the pressure at a general position x, y, z and at time t . In addition, we assume a gas law of the form:

$$p = p(\rho) \quad (3)$$

OPERATOR SPLITTING

We solve (1) using a Riemann solver which we develop shortly, together with the technique of operator splitting⁶, i.e. we solve successively:

$$\mathbf{w}_t + \mathbf{F}_x = \mathbf{0} \quad (4a)$$

$$\mathbf{w}_t + \mathbf{G}_y = \mathbf{0} \quad (4b)$$

and

$$\mathbf{w}_t + \mathbf{H}_z = \mathbf{0} \quad (4c)$$

along x -, y - and z -coordinate lines, respectively.

We give the scheme for the solution of (4a) and the scheme for the solution of (4b) and (4c) will then follow by symmetry.

LINEARIZED RIEMANN PROBLEM

If the approximate solution of (4a) is sought along a line $y = y_0, z = z_0$ using a finite difference method, then the solution is known at a set of discrete mesh points $(x, y, z, t) = (x_j, y_0, z_0, t_n)$ at any time $t = t_n$. Following Godunov⁷ the approximate solution \mathbf{w}_j^n to \mathbf{w} at (x_j, y_0, z_0, t_n) can be considered as a set of piecewise constants $\mathbf{w} = \mathbf{w}_j^n$ for $x \in \left(x_j - \frac{\Delta x}{2}, x_j + \frac{\Delta x}{2}\right)$ at time t_n where

$\Delta x = x_j - x_{j-1}$ is a constant mesh spacing. A Riemann problem is now present at each interface $x_{j-1/2} = \frac{1}{2}(x_{j-1} + x_j)$ separating adjacent states $\mathbf{w}_{j-1}^n, \mathbf{w}_j^n$. If (4a) is linearized by considering the Jacobian matrix of the flux function \mathbf{F} to be constant in each interval (x_{j-1}, x_j) , the resulting equations can be solved approximately using explicit time stepping. The time step Δt is restricted so that the solutions of adjacent Riemann problems do not interact. The scalar problems that result from this analysis can be solved by upwind differencing; however, an approximate Jacobian matrix needs to be constructed in each interval so that shock-capturing is automatic.

APPROXIMATE RIEMANN SOLVER

Structure

The Jacobian matrix:

$$A = \frac{\partial \mathbf{F}}{\partial \mathbf{w}} = \begin{bmatrix} 0 & 1 & 0 & 0 \\ a^2 - u^2 & 2u & 0 & 0 \\ -uv & v & u & 0 \\ -uw & w & 0 & u \end{bmatrix} \quad (5)$$

of the flux function $\mathbf{F}(\mathbf{w})$ has eigenvalues λ_i with corresponding eigenvectors \mathbf{e}_i , $i = 1, 2, 3, 4$ given by:

$$\lambda_1 = u + a \quad \mathbf{e}_1 = (1, u + a, v, w)^T \quad (6a)$$

$$\lambda_2 = u - a \quad \mathbf{e}_2 = (1, u - a, v, w)^T \quad (6b)$$

$$\lambda_3 = u \quad \mathbf{e}_3 = (0, 0, 1, 0)^T \quad (6c)$$

$$\lambda_4 = u \quad \mathbf{e}_4 = (0, 0, 0, 1)^T \quad (6d)$$

where the sound speed a is given by:

$$a^2 = dp(\rho)/d\rho \quad (6a)$$

using the gas law (3). This information can be used to develop approximate solutions of the Riemann problem in the previous section.

Shock capturing

Consider two adjacent states $\mathbf{w}_L, \mathbf{w}_R$ (left and right) given at either end of the cell (x_L, x_R) on an x -coordinate line $y = y_0, z = z_0$ and consider also the algebraic problem of finding an approximate Jacobian $\tilde{A} = \tilde{A}(\mathbf{w}_L, \mathbf{w}_R)$ in this cell such that:

$$\tilde{A} \Delta \mathbf{w} = \Delta \mathbf{F} \quad (7)$$

where $\Delta(\cdot) = (\cdot)_R - (\cdot)_L$, $\mathbf{w} = (\rho, \rho u, \rho v, \rho w)^T$ and $\mathbf{F} = (\rho u, p + \rho u^2, \rho uv, \rho uw)^T$. A solution to this problem, for arbitrary jumps $\Delta \mathbf{w}$, can be used to obtain a conservative scheme with good shock-capturing properties.

Construction of \tilde{A}

To determine the matrix \tilde{A} we first write $\Delta \mathbf{w}$ and $\Delta \mathbf{F}$ in terms of $\Delta \mathbf{u}$, where $\mathbf{u} = (\rho, u, v, w)^T$ can be thought of as a parameter or intermediate vector³. Following the identities:

$$\Delta \rho = \Delta \rho \quad (8)$$

$$\Delta(\rho U) = \bar{\rho} \Delta U + \bar{U} \Delta \rho, \quad U = u, v, w \quad (9a-c)$$

where

$$\bar{\rho} = \frac{1}{2}(\rho_L + \rho_R) \quad (10)$$

$$\bar{U} = \frac{1}{2}(U_L + U_R) \quad U = u, v, w \quad (11a-c)$$

the arithmetic mean of left and right states, we can write:

$$\Delta \mathbf{w} = \tilde{B} \Delta \mathbf{u} \quad (12)$$

where

$$\tilde{B} = \begin{pmatrix} 1 & 0 & 0 & 0 \\ \bar{u} & \bar{\rho} & 0 & 0 \\ \bar{v} & 0 & \bar{\rho} & 0 \\ \bar{w} & 0 & 0 & \bar{\rho} \end{pmatrix} \quad (13)$$

Similarly,

$$\Delta(\rho U^2) = \bar{U}^2 \Delta\rho + \bar{\rho} \Delta U^2 = \bar{U}^2 \Delta\rho + 2\bar{\rho} \bar{U} \Delta U \quad (14a-c)$$

where

$$\bar{U}^2 = \frac{1}{2}(U_L^2 + U_R^2), \quad U = u, v, w \quad (15a-c)$$

the arithmetic mean of the square of the velocity components, and:

$$\Delta p = \tilde{a}^2 \Delta\rho \quad (16)$$

where

$$\tilde{a}^2 = \begin{cases} \frac{\Delta p}{\Delta\rho} & \text{if } \Delta\rho \neq 0, \rho_L \neq \rho_R \\ \frac{dp(\rho)}{d\rho} & \text{if } \Delta\rho = 0, \rho_L = \rho_R = \rho \end{cases} \quad (17a-b)$$

Finally

$$\Delta(\rho uv) = \overline{uv} \Delta\rho + \bar{\rho} \bar{v} \Delta u + \bar{\rho} \bar{u} \Delta v \quad (18)$$

and

$$\Delta(\rho uw) = \overline{uw} \Delta\rho + \bar{\rho} \bar{w} \Delta u + \bar{\rho} \bar{u} \Delta w \quad (19b)$$

where

$$\overline{uv} = \frac{1}{2}(u_L v_L + u_R v_R) \quad (19a)$$

and

$$\overline{uw} = \frac{1}{2}(u_L w_L + u_R w_R) \quad (19b)$$

and $\bar{\rho}$, \bar{u} , \bar{v} , \bar{w} are given above (N.B. The choice in (18a-b) is made so that the eigenvalues of the approximate Jacobian \tilde{A} have the simplest possible form. In particular, \tilde{A} has \bar{u} as two eigenvalues.) Combining (9a-c), (14a-c), (16) and (18a-b) gives:

$$\Delta \mathbf{F} = \tilde{C} \Delta \mathbf{u} \quad (20)$$

where

$$\tilde{C} = \begin{pmatrix} \bar{u} & \bar{\rho} & 0 & 0 \\ \overline{u^2} + \tilde{a}^2 & 2\bar{\rho}\bar{u} & 0 & 0 \\ \overline{uv} & \bar{\rho}\bar{v} & \bar{\rho}\bar{u} & 0 \\ \overline{uw} & \bar{\rho}\bar{w} & 0 & \bar{\rho}\bar{u} \end{pmatrix} \quad (21)$$

and thus from (12) and (20):

$$\Delta \mathbf{F} = \tilde{C} \tilde{B}^{-1} \Delta \mathbf{w} \quad (22)$$

Therefore a solution of (7) is obtained with the approximate Jacobian:

$$\tilde{A} = \tilde{C}\tilde{B}^{-1} = \begin{pmatrix} 0 & 1 & 0 & 0 \\ \tilde{a}^2 + \bar{u}^2 - 2\bar{u}^2 & 2\bar{u} & 0 & 0 \\ \bar{uv} - 2\bar{u}\bar{v} & \bar{v} & \bar{u} & 0 \\ \bar{uw} - 2\bar{u}\bar{w} & \bar{w} & 0 & \bar{u} \end{pmatrix} \tag{23}$$

The terms $\bar{u}^2 - 2\bar{u}^2$, $\bar{uv} - 2\bar{u}\bar{v}$ and $\bar{uw} - 2\bar{u}\bar{w}$ in \tilde{A} can be simplified, however, since:

$$\bar{u}^2 - 2\bar{u}^2 = \frac{1}{2}(u_L^2 + u_R^2) - 2\left(\frac{1}{2}(u_L + u_R)\right)^2 = -u_L u_R = -\hat{u}^2 \tag{24}$$

where

$$\hat{u} = \sqrt{u_L u_R} \tag{25}$$

is the geometric mean of left and right states, and

$$\begin{aligned} \bar{uv} - 2\bar{u}\bar{v} &= \frac{1}{2}(u_L v_L + u_R v_R) - 2\left[\frac{1}{2}(u_L + u_R)\right]\left[\frac{1}{2}(v_L + v_R)\right] \\ &= -\frac{1}{2}(u_L v_R + u_R v_L) = -\tilde{uv} \end{aligned} \tag{26}$$

say. Similarly,

$$\bar{uw} - 2\bar{u}\bar{w} = -\frac{1}{2}(u_L w_R + u_R w_L) = -\tilde{uw} \tag{26}$$

Hence

$$\tilde{A} = \begin{pmatrix} 0 & 1 & 0 & 0 \\ \tilde{a}^2 - \hat{u}^2 & 2\bar{u} & 0 & 0 \\ -\tilde{uv} & \bar{v} & \bar{u} & 0 \\ -\tilde{uw} & \bar{w} & 0 & \bar{u} \end{pmatrix} \tag{27}$$

is the required average Jacobian satisfying (6a), with $\bar{\rho}$, \bar{u} , \bar{v} , \hat{u} , \bar{w} , \tilde{a}^2 , \tilde{uv} and \tilde{uw} given by (10), (11a-c), (16), (25) and (26a-b). Clearly, as $w_L, w_R \rightarrow w$ then $\tilde{A} \rightarrow A$, the continuous Jacobian.

Approximate eigenvalues and eigenvectors

Now, the important quantities that are needed for the scheme are the eigenvalues $\tilde{\lambda}_i$ and eigenvectors \tilde{e}_i of \tilde{A} , and it is a simple matter to show that these are given by:

$$\tilde{\lambda}_{1,2,3,4} = \bar{u} \pm \tilde{a}, \bar{u}, \bar{u} \tag{28a-d}$$

$$\tilde{e}_{1,2} = \left(1, \bar{u} \pm \tilde{a}, \bar{v} \pm \frac{1}{4} \frac{\Delta u \Delta v}{\tilde{a}}, \bar{w} \pm \frac{1}{4} \frac{\Delta u \Delta w}{\tilde{a}} \right)^T \tag{29a-b}$$

$$\tilde{e}_3 = (0, 0, 1, 0)^T \tag{29c}$$

and

$$\tilde{e}_4 = (0, 0, 0, 1)^T \tag{29d}$$

where

$$\tilde{a} = (\hat{a}^2 + \frac{1}{4}(\Delta u)^2)^{1/2} \tag{30}$$

(We have used the identities $\bar{u}^2 - \hat{u}^2 = \frac{1}{4}(\Delta u)^2$, $\bar{uv} - \tilde{uv} = \bar{uv} - \bar{u}\bar{v} = \frac{1}{4}\Delta u \Delta v$ and $\bar{uw} - \tilde{uw} = \bar{uw} - \bar{u}\bar{w} = \frac{1}{4}\Delta u \Delta w$ in determining these.)

Projection

Finally, it is necessary to project a general jump Δw onto the eigenvectors \tilde{e}_i as:

$$\Delta w = \sum_{i=1}^4 \tilde{\alpha}_i \tilde{e}_i \tag{31}$$

and by virtue of (6a) we then have:

$$\Delta F = \sum_{i=1}^4 \tilde{\lambda}_i \tilde{\alpha}_i \tilde{e}_i \tag{32}$$

Solving (7) gives:

$$\tilde{\alpha}_{1,2} = \frac{1}{2} \left(\Delta \rho \pm \frac{\tilde{\rho}}{\tilde{a}} \Delta u \right) \tag{33a-b}$$

$$\tilde{\alpha}_3 = \frac{\tilde{\rho} \tilde{a}^2}{\tilde{a}^2} \Delta v \tag{33c}$$

and

$$\tilde{\alpha}_4 = \tilde{\rho} \frac{\tilde{a}^2}{\tilde{a}^2} \Delta w \tag{33d}$$

Numerical scheme

Thus in (4a) we can approximate:

$$F_x \sim \frac{\Delta F}{\Delta x} = \tilde{A} \frac{\Delta F}{\Delta x} = \tilde{A} \frac{\sum_{i=1}^4 \tilde{\alpha}_i e_i}{\Delta x} = \frac{\sum_{i=1}^4 \tilde{\lambda}_i \tilde{\alpha}_i \tilde{e}_i}{\Delta x} \tag{34a}$$

by virtue of the analysis of this section. Applying upwind differencing to (4a) using the approximation in (34a) then gives:

$$\frac{w_j^{n+1} - w_j^n}{\Delta t} + \frac{\left(\sum_{i=1}^4 \tilde{\lambda}_i^+ \tilde{\alpha}_i \tilde{e}_i \right)_{j-1/2}}{\Delta x} + \frac{\left(\sum_{i=1}^4 \tilde{\lambda}_i^- \tilde{\alpha}_i \tilde{e}_i \right)_{j+1/2}}{\Delta x} = 0 \tag{34b}$$

refers to the cell $[x_{j-1}, x_j]$ and

$$\tilde{\lambda}_i^\pm = \frac{1}{2} (\tilde{\lambda}_i \pm |\tilde{\lambda}_i|) \tag{35}$$

represent the positive and negative parts of $\tilde{\lambda}_i$. This gives the following first order algorithm for the solution of (4a):

$$\left. \begin{array}{l} \text{add } -\frac{\Delta t}{\Delta x} \tilde{\lambda}_i \tilde{\alpha}_i \tilde{e}_i \text{ to } w_R \text{ when } \tilde{\lambda}_i > 0 \\ \text{or} \\ \text{add } -\frac{\Delta t}{\Delta x} \tilde{\lambda}_i \tilde{\alpha}_i \tilde{e}_i \text{ to } w_L \text{ when } \tilde{\lambda}_i < 0 \end{array} \right\} \tag{36}$$

Hence the only quantities required for the algorithm are:

$$\begin{aligned} \tilde{\lambda}_{1,2,3,4} &= \bar{u} \pm \bar{a}, \bar{u}, \bar{u} \\ \tilde{\mathbf{e}}_{1,2} &= \left(1, \bar{u} \pm \bar{a}, \bar{v} \pm \frac{1}{4} \frac{\Delta u \Delta v}{\bar{a}}, \bar{w} \pm \frac{1}{4} \frac{\Delta u \Delta w}{\bar{a}} \right)^T \\ \tilde{\mathbf{e}}_3 &= (0, 0, 1, 0)^T \\ \tilde{\mathbf{e}}_4 &= (0, 0, 0, 1)^T \\ \tilde{\alpha}_{1,2} &= \frac{1}{2} \left(\Delta \rho \pm \frac{\bar{\rho}}{\bar{a}} \Delta u \right) \\ \tilde{\alpha}_3 &= \frac{\bar{\rho} \tilde{a}^2}{\bar{a}^2} \Delta v \\ \tilde{\alpha}_4 &= \frac{\bar{\rho} \tilde{a}^2}{\bar{a}^2} \Delta w \end{aligned}$$

where

$$\begin{aligned} \bar{U} &= \frac{1}{2}(U_L + U_R), \quad U = u, v, w \\ \bar{\rho} &= \frac{1}{2}(\rho_L + \rho_R) \end{aligned}$$

and

$$\tilde{a} = (\bar{a}^2 + \frac{1}{4}(\Delta u)^2)^{1/2}$$

so that only one square root is taken in each computational cell. Thus, we note the direction of flow of information given by the approximate eigenvalues $\tilde{\lambda}_i$ and use this information to update the solution consistent with the theory of characteristics of (1). In addition, second order transfers of these first order increments can be made to achieve higher accuracy, providing they are limited to maintain monotonicity⁸. The use of these ‘flux-limiters’ improves accuracy without introducing non-physical spurious oscillations, especially at shocks. A similar analysis applies for the scheme for solving (4b–c).

Finally, to avoid entropy-violating solutions, the first order increment can be considered as two separate increments being sent to either end of the cell. Specifically, the modified version of the scheme can be written cell-wise as:

$$w_{j-1}^{n+1} = w_{j-1}^n + \frac{\Delta t}{\Delta x} \tilde{\sigma}_i^L \tilde{\alpha}_i \tilde{\mathbf{e}}_i \quad i = 1, 2, 3, 4 \tag{37a}$$

$$w_j^{n+1} = w_j^n + \frac{\Delta t}{\Delta x} \tilde{\sigma}_i^R \tilde{\alpha}_i \tilde{\mathbf{e}}_i \tag{37b}$$

where

$$\tilde{\sigma}_i^L = \begin{cases} (-\tilde{\lambda}_i)^+ & \tilde{\lambda}_i^R = \tilde{\lambda}_i^L \\ \frac{(-\tilde{\lambda}_i^R)^+ (\tilde{\lambda}_i - \tilde{\lambda}_i^L) + (-\tilde{\lambda}_i^L)^+ (\tilde{\lambda}_i^R - \tilde{\lambda}_i)}{\tilde{\lambda}_i^R - \tilde{\lambda}_i^L} & \tilde{\lambda}_i^R \neq \tilde{\lambda}_i^L \end{cases} \tag{38b}$$

and

$$\tilde{\sigma}_i^L = \begin{cases} -(\tilde{\lambda})^+ & \tilde{\lambda}_i^R = \tilde{\lambda}_i^L \\ \frac{-(\tilde{\lambda}_i^R)^+ (\tilde{\lambda}_i - \tilde{\lambda}_i^L) - (\tilde{\lambda}_i^L)^+ (\tilde{\lambda}_i^R - \tilde{\lambda}_i)}{\tilde{\lambda}_i^R - \tilde{\lambda}_i^L} & \tilde{\lambda}_i^R \neq \tilde{\lambda}_i^L \end{cases} \tag{38c}$$

$$\tag{38d}$$

The expressions $\tilde{\lambda}_i^L, \tilde{\lambda}_i^R$ are given by:

$$\tilde{\lambda}_i^L = \min(j_{-1/2}\tilde{\lambda}_i, j_{-3/2}\tilde{\lambda}_i) \tag{39a}$$

$$\tilde{\lambda}_i^R = \max(j_{-1/2}\tilde{\lambda}_i, j_{+1/2}\tilde{\lambda}_i) \tag{39b}$$

where $j_{-1/2}\tilde{\lambda}_i \equiv \tilde{\lambda}_i$, and these will be different for a rarefaction wave.

EXTENSIONS

Employing the familiar gas-dynamics analogy, the two-dimensional form of (1)–(3) give rise to the shallow water equations, viz.:

$$\mathbf{w}_t + \mathbf{F}_x + \mathbf{G}_y = \mathbf{f} + \mathbf{g} \tag{40}$$

where

$$\mathbf{w} = (\rho, \rho u, \rho v)^T \tag{41a}$$

$$\mathbf{F} = (\rho u, \rho^2/2 + \rho u^2, \rho uv)^T \tag{41b}$$

$$\mathbf{G} = (\rho v, \rho vu, \rho^2/2 + \rho v^2)^T \tag{41c}$$

and the ‘gas law’ $p = \frac{1}{2}\rho^2$ has been used. The quantities ρ, u and v denote g multiplied by the height of water above the bottom of a channel of undisturbed depth $h(x, y)$, and the velocity components of the fluid, where g is the acceleration due to gravity. In addition, the source terms \mathbf{f}, \mathbf{g} (associated with the x - and y -directions, respectively) are given by:

$$\mathbf{f} = (0, g\rho(h_x - s_x), 0)^T \tag{42a}$$

and

$$\mathbf{g} = (0, 0, g\rho(h_y - s_y))^T \tag{42b}$$

where the quantities s_x, s_y are the slopes of the energy grade lines in the x - and y -directions, respectively, and are determined from the steady-state friction formulae:

$$s_x = \frac{n^2 u \sqrt{u^2 + v^2}}{(\rho/g)^{1/2}} \tag{43a}$$

$$s_y = \frac{n^2 v \sqrt{u^2 + v^2}}{(\rho/g)^{1/2}} \tag{43b}$$

where n represents Manning’s roughness coefficient.

Equation (40) can be solved using the algorithm of the previous section with the modification that (4a) is replaced by:

$$\mathbf{w}_t + \mathbf{F}_x = \mathbf{f} \tag{44a}$$

and similarly, (4b) is replaced by:

$$\mathbf{w}_t + \mathbf{G}_y = \mathbf{g} \tag{44b}$$

(Note that the quantity \tilde{a}^2 given by (17a) becomes:

$$\tilde{a}^2 = \frac{1}{2} \frac{(\rho_R^2 - \rho_L^2)}{\rho_R - \rho_L} = \frac{1}{2} (\rho_L + \rho_R) = \bar{\rho} \tag{44c}$$

which is consistent with the form in (17b) when $\rho_L = \rho_R$.)

We follow the approach in Reference 1 and unwind the source term \mathbf{f} . Specifically,

approximating \mathbf{f} in the interval (x_L, x_R) by $\tilde{\mathbf{f}} = \left(0, g\bar{\rho}\left(\frac{\Delta h}{\Delta x} - \tilde{s}_x\right), 0\right)^T$ where $\bar{\rho} = \frac{1}{2}(\rho_L + \rho_R)$,

$\Delta h = h(x_R, y_0) - h(x_L, y_0)$, $\tilde{s}_x = \frac{n^2\bar{u}\sqrt{\bar{u}^2 + \bar{v}^2}}{(\bar{\rho}/g)^{4/3}}$ and projecting:

$$\tilde{\mathbf{f}} = -\frac{1}{\Delta x} \sum_{i=1}^3 \tilde{\lambda}_i \tilde{\beta}_i \tilde{\mathbf{e}}_i \quad (45)$$

enables (44a) to be solved approximately. The first order algorithm can be written as in (36) where the $\tilde{\alpha}_i$ are replaced by modified wavestrengths $\tilde{\gamma}_i = \tilde{\alpha}_i + \tilde{\beta}_i$.

TEST PROBLEM

This is a two-dimensional dam break problem with a non-symmetrical breach. The equations of flow are the two-dimensional isentropic equations where the gas dynamics analogy with the shallow water equations has been employed (see above). The computational domain is defined by a channel 200 m long \times 200 m wide and the non-symmetrical breach is 75 m and the dam is 10 m thick, as shown in *Figure 1*. Initially, the water is at different heights ρ_0, ρ_1 either side of the breach. For comparison purposes with other algorithms we consider a horizontal, frictionless channel.

NUMERICAL RESULTS

Two sets of initial conditions are chosen here: (a) $\rho_1/g = 10$, $\rho_0/g = 5$; and (b) $\rho_1/g = 10$, $\rho_0/g = 0.05$, representing tailwater/reservoir height ratios of 0.5 and 0.005 respectively. The 'Minmod' limiter⁸ has been used and a grid of 41×41 points results in a mesh size of 5 m by

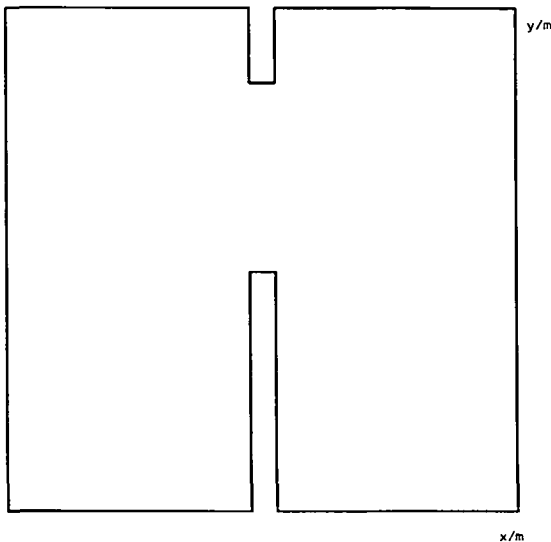


Figure 1 The computational domain

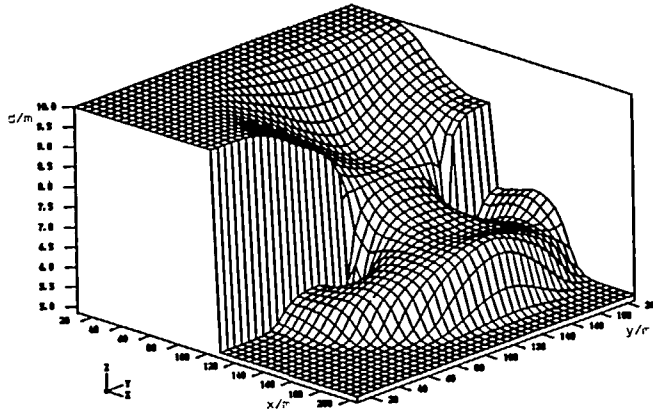


Figure 2 Contours of surface elevation for tailwater reservoir height ratio 0.5 at time 7.1 s

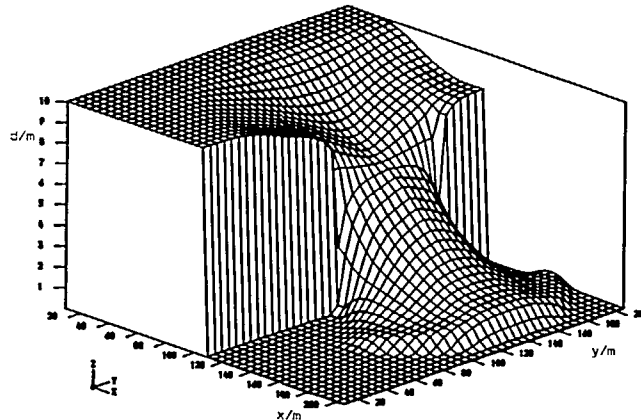


Figure 3 Contours of surface elevation for tailwater/reservoir height ratio 0.005 at time 7.1 s

5 m. The results displaying surface elevation contours for these two cases are shown in *Figures 2 and 3*, respectively, at time $t = 7.1$ s. (N.B. The Figures display contours where the dam is still intact since it is not possible to mask these areas.) In both cases we see that the bore has developed well. Only in case (a) is there significant reflection from the wall. This compares favourably with the results where the bore is smeared over a number of cells^{4,5}. It is noted by Fennema and Chaudry⁵ that many numerical schemes have difficulty in computing accurate solutions, if any, for small ratios of tailwater/reservoir height. We note, however, in computing these satisfactory results that we have not expended a great deal of effort in respect of computer time used, or even in storage requirements, merely the use of an efficient approximate Riemann solver. The results are also in agreement with those obtained by Glaister¹. Using an Amdahl V7 with 41×41 mesh points and the 'Minmod' limiter takes 0.26 cpu seconds to compute one time step and a total of 9.1 cpu seconds to reach a real time of 7.1 s using 35 time steps.

The boundary conditions at inflow are prescribed as the initial conditions, whilst on outflow all information is leaving the computational domain and therefore nothing has to be done. At rigid walls we employ reflecting boundary conditions, i.e. mesh points, and the resulting cell,

straddle a rigid wall boundary, and the surface elevation/density (and tangential velocity) is prescribed to be the same at each end of such a cell; whereas the normal velocity has the same magnitude, but opposite sign, at each end of such a cell. This enables the boundary conditions to be overwritten along rigid wall boundaries.

CONCLUSIONS

A conservative finite difference scheme is presented for the solution of the three-dimensional equations of isentropic flow based on flux difference splitting. By considering linearized Riemann problems, and solving these approximately using upwind differencing, enables the flow resulting from a dam-break to be predicted accurately. In particular, the use of particular cell averages of flow variables results in correct shock/bore speeds being attained, together with bore heights, and the resulting scheme is computationally efficient through the use of arithmetic averaging.

REFERENCES

- 1 Glaister, P. Flux differencing splitting for open channel flows, *Int. J. Num. Meth. Fluids*, **16**, 629 (1993)
- 2 Glaister, P. An approximate linearised Riemann solver for the one-dimensional Euler equations with real gases, *J. Comp. Phys.*, **74**, 382–408 (1988)
- 3 Roe, P. L. Approximate Riemann solvers, parameter vectors and difference schemes, *J. Comp. Phys.*, **43**, 357 (1981)
- 4 Fennema, R. J. and Chaudry, M. H. Simulation of one-dimensional dam-break flows, *J. Hyd. Res.*, **25**, 41–51 (1987)
- 5 Fennema, R. J. and Chaudry, M. H. Implicit methods for two-dimensional unsteady free-surface flows, *J. Hyd. Res.*, **27**, 321–332 (1989)
- 6 Yanenko, N. N. *The Method of Fractional Steps*, Springer-Verlag; Berlin (1971)
- 7 Godunov, S. K. A difference method for the numerical computation of continuous solutions of hydrodynamic equations, *Mat. Sbornik*, **47**, 271–306 (1959) [Translated as *JPRS 7225* by US Dept. of Commerce (1960)]
- 8 Sweby, P. K. High resolution schemes using flux limiters for hyperbolic conservation laws, *SIAM J. Num. Anal.*, **21**, 995 (1984)